

\mathbb{Z}_N symmetry breaking in Projected Entangled Pair State models

Manuel Rispler,^{1,2} Kasper Duivenvoorden,² and Norbert Schuch¹

¹*Max-Planck-Institute of Quantum Optics, Hans-Kopfermann-Str. 1, 85748 Garching, Germany*

²*JARA Institute for Quantum Information, RWTH Aachen University, 52056 Aachen, Germany*

We consider Projected Entangled Pair State (PEPS) models with a global \mathbb{Z}_N symmetry, which are constructed from \mathbb{Z}_N -symmetric tensors and are thus \mathbb{Z}_N -invariant wavefunctions, and study the occurrence of long-range order and symmetry breaking in these systems. First, we show that long-range order in those models is accompanied by a degeneracy in the so-called transfer operator of the system. We subsequently use this degeneracy to determine the nature of the symmetry broken states, i.e., those stable under arbitrary perturbations, and provide a succinct characterization in terms of the fixed points of the transfer operator (i.e. the different boundary conditions) in the individual symmetry sectors. We verify our findings numerically through the study of a \mathbb{Z}_3 -symmetric model, and show that the entanglement Hamiltonian derived from the symmetry broken states is quasi-local (unlike the one derived from the symmetric state), reinforcing the locality of the entanglement Hamiltonian for gapped phases.

I. INTRODUCTION

Spontaneous symmetry breaking is a prime example of the emergence of global order from local interactions in quantum systems at zero temperature. The formation of macroscopic domains in which a single ordered state is selected from a set of energetically equivalent states is witnessed by the onset of long-range order, i.e., non-decaying two-point correlations. In any finite system, the ground space of a symmetric Hamiltonian is an irreducible representation, and therefore unique for any Abelian symmetry. Long range order implies the existence of low lying excited states [1, 2] for which the gap closes in the thermodynamic limit. The physical ground states are then those which are stable under general (symmetry breaking) perturbations of the Hamiltonian; they turn out to be hybridizations of the symmetric and low lying excited states and therefore break the symmetry of the system.

Projected Entangled Pair States (PEPS) form a framework for modelling the low-energy states of interacting quantum systems. The central object here is a local tensor which is being used to build up global wavefunctions locally, based on their entanglement structure. PEPS thus form the right ansatz to approximate the low-energy physics of systems governed by local interactions [3, 4], making them a powerful tool for the variational simulation of interacting many-body systems [5, 6]. At the same time, PEPS form a versatile analytical framework: Since every PEPS is the exact ground state of an associated parent Hamiltonian [7] which inherits all symmetries from the tensor, they can be used to construct solvable models where the desired physical structure is built directly into the tensor. A particularly appealing feature of PEPS models is that they allow to explicitly identify the degrees of freedom associated to the entanglement spectrum and the edge physics of the system. Thereby, they clarify the nature of the one-dimensional system underlying both edge physics and entanglement properties, and allow to explicitly determine the one-dimensional entan-

glement Hamiltonian [8, 9].

Despite their construction from local tensors, PEPS models can naturally describe systems with emergent global order, such as systems with topological entanglement, or systems which exhibit long-range order and thus spontaneous symmetry breaking [10]. Yet, in the scenario of spontaneous symmetry breaking the PEPS tensor, which encodes the local physics of the system, will clearly be invariant under the respective symmetry, and thus will also be the global PEPS wavefunction. This is, while the system exhibits long-range order, the wavefunction does not actually break the symmetry, which is reflected in unphysical cat-like states in the entanglement spectrum of the system. Thus, the question arises how to understand the occurrence of spontaneous symmetry breaking in PEPS models with long-range order, and in particular how to obtain the symmetry broken wavefunctions and the corresponding edge states and entanglement spectra and Hamiltonians.

In this paper, we study the occurrence of symmetry breaking for PEPS models with an abelian \mathbb{Z}_N symmetry. Specifically, we address two questions: First, we show how long-range order in a PEPS model is accompanied by a degeneracy in the so-called transfer operator, and second, we use this degeneracy to determine the structure of the symmetry broken states, i.e., those ground states which are stable under perturbations. We then apply our results to study the entanglement Hamiltonian, where we observe that the symmetry broken states allow to restore the locality of the entanglement Hamiltonian in the symmetry broken phase.

More specifically, we start by considering a system with long-range order, which generally implies the presence of symmetry breaking. In PEPS, the so-called transfer operator (describing a one-dimensional slice of the system) mediates all correlation functions. We prove that the presence of long-range order implies an approximate degeneracy in the spectrum of the transfer operator, labelled by symmetry sectors, which becomes exact in the thermodynamic limit. The different fixed points of the transfer operator correspond to different states in the

ground space manifold of the system. We then consider the behavior of the transfer operator under physical perturbations of the model (i.e., those corresponding to perturbations of its Hamiltonian). Using the algebraic structure of the fixed point space, we are able to succinctly characterize the stable fixed points, and we find that there is a unique set of stable fixed points, given by the Fourier transform of the fixed points in the individual irrep sectors. These stable fixed points provide the boundary conditions which yield the symmetry broken states. At the same time, any fixed point also provides direct access to the entanglement spectrum of the systems [8]. We use this to derive the entanglement Hamiltonian both for the symmetric and the symmetry broken ground states, and find that the locality of the entanglement Hamiltonian is restored by choosing the symmetry broken states. This reinforces the perspective that the entanglement Hamiltonian is local for any gapped phase [8, 11].

We have initiated the study of PEPS with symmetry breaking and long-range order in Ref. [12], where we have considered the special case of a broken \mathbb{Z}_2 symmetry, related it to the transfer operator spectrum, and determined the stable fixed points. In the present work, we generalize this to the case of \mathbb{Z}_N symmetries, to which end we in particular establish entirely different proof techniques in order to characterize the stable fixed points, based on the algebra structure of the fixed point space of the transfer operator. The present approach also goes beyond Ref. [12] in that it no longer requires Hermiticity of the transfer operator.

The paper is structured as follows: In Sec. II, we introduce the necessary tools to study PEPS models. In Sec. III we review and extend the arguments of Ref. [12] to show that long range order implies a degeneracy in the transfer operator. In Sec. IV we show which of these fixed points model stable environments. These stable fixed points can be obtained from symmetric fixed points by a Fourier transform. In Sec. V we perform a numerical study of a family of \mathbb{Z}_3 -symmetric PEPS models related to the \mathbb{Z}_3 Potts model to verify the stability of the earlier defined stable fixed points, and demonstrate that the entanglement Hamiltonian arising from stable fixed points is quasi-local.

II. PROJECTED ENTANGLED PAIR STATE MODELS

Let us introduce PEPS. We will, w.l.o.g., work on a square lattice of size $N_v \times N_h$. The model is defined by the five-index tensor $A_{\alpha\beta\gamma\delta}^i$ with the *physical* index $i = 0 \dots d - 1$, where d is the physical dimension of each site and the *auxiliary* indices $\alpha, \beta, \gamma, \delta = 0 \dots D - 1$ with the so called *bond dimension* D . This tensor could be site dependent, but to ease notation, we stick with a single site independent tensor and in doing so only consider translational invariant models. The wave function

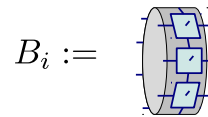


FIG. 1. Definition of the B_i tensor, where all left virtual indices, all physical indices and all right virtual indices are each viewed as the respective composite indices of an MPS tensor.

can be constructed by putting one tensor on each site of the lattice and contracting all *auxiliary* indices. One could either decide to model periodic boundary conditions (contract indices on opposite edges) or model open boundary conditions by an extra boundary tensor. The remaining, *physical* indices constitute the coefficients of the wavefunction as $|\Psi\rangle = \sum c_{i_1 \dots i_{(N_v N_h)}} |i_1 \dots i_{(N_v N_h)}\rangle$.

We will assume the tensor $A_{\alpha\beta\gamma\delta}^i$ to be symmetric under a \mathbb{Z}_N symmetry generated by unitary S and s in the following manner:

$$\sum_j s_{ij} A_{\alpha\beta\gamma\delta}^j = \sum_{\alpha'\beta'\gamma'\delta'} A_{\alpha'\beta'\gamma'\delta'}^i S_{\alpha\alpha'} S_{\beta\beta'} S_{\gamma'\gamma}^\dagger S_{\delta'\delta}^\dagger. \quad (1)$$

It is straightforward to see that the global wave function is invariant as $s^{\otimes (N_v N_h)} |\psi\rangle = |\psi\rangle$ in case of periodic boundary conditions. The PEPS tensors A not only give rise to a wave function, but also to a parent Hamiltonian which has this wave function as its ground state, and moreover commutes with a global action of the symmetry s . In order to define the parent Hamiltonian, let \mathcal{A} be a linear map from the auxiliary space to the physical space, $\mathcal{A} : (\mathbb{C}^D)^{\otimes 4} \rightarrow \mathbb{C}^d$, related to the PEPS as $\mathcal{A} = \sum A_{\alpha\beta\gamma\delta}^i |i\rangle \langle \alpha\beta\gamma\delta|$. Similarly, for any region R one can construct the linear map \mathcal{A}_R from the boundary auxiliary space of R to the bulk physical space of R by taking $|R|$ copies of \mathcal{A} and contracting the inner indices. The parent Hamiltonian is given by $H = \sum_R h_R$ where h_R acts as the projector on the orthogonal complement of the image of \mathcal{A}_R . The sum runs for example over all R forming a 2 by 2 patch. From the symmetry of A , all maps \mathcal{A}_R are also symmetric and hence also their image, showing that the parent Hamiltonian is also symmetric.

For the rest of this article we will assume periodic boundary conditions in the vertical (y) direction, thus either toric or cylindrical topology. By blocking the tensors corresponding to each vertical slice of the lattice into one composite tensor B_i , Fig. 1, the state formally becomes a matrix product state (MPS). The transfer operator for such states is a completely positive map defined as $\mathbb{T}(\rho) := \sum_i B^i \rho (B^i)^\dagger$. Similar to the MPS case, it can be used to calculate wave function overlaps and expectation values. For example let O and O' be two operators acting on sites $i = (i_x, i_y)$ and $j = (j_x, j_y)$, with $i_x < j_x$. Let $\mathbb{T}_O^{[k]}$ be the mixed transfer matrix obtained by inserting an operator O between the local tensors A and A^\dagger corresponding to the k -th site: $\mathbb{T}_O^{[k]} := \sum_{ij} B^j \rho (B^i)^\dagger O_{ij}^{[k]}$, see Fig. 2.

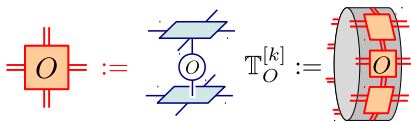


FIG. 2. Definition of the dressed transfer operator $\mathbb{T}^{[k]}$, the operator acts on physical level on site $[k]$ (site label omitted in figure).

Then we have that

$$\langle O_i O'_j \rangle = \frac{\text{Tr} \left[l^\dagger \mathbb{T}^{d_1} \mathbb{T}_O^{[i_y]} \mathbb{T}^{d_2} \mathbb{T}_{O'}^{[j_y]} \mathbb{T}^{d_3}(r) \right]}{\text{Tr} \left[l^\dagger \mathbb{T}^{N_h}(r) \right]}, \quad (2)$$

with $d_1 = i_x - 1$, $d_2 = j_x - i_x - 1$ and $d_3 = N_h - j_x$ and l and r some boundary tensors. From this expression we see that, just as in the one dimensional case, all correlations between observables on different horizontal sites are controlled by the spectral properties of the transfer operator. A new feature in two dimensions is that this transfer operator now has itself a one dimensional structure, which as we will see later allows for criticality and phase transitions. These features do not arise in the one dimensional MPS case, where correlations are guaranteed to decay exponentially since \mathbb{T} is independent of system size.

The symmetry of the tensor A carries over to the Kraus operators B_i of the transfer operator, $\sum_i u_{ij} B_j = U B_i U^\dagger$, and hence to the transfer operator:

$$U \mathbb{T}(\rho) U^\dagger = \mathbb{T}(U \rho U^\dagger), \quad (3)$$

where $U = S^{\otimes N_v}$ and $u = s^{\otimes N_v}$. The eigenvectors of \mathbb{T} can thus be labeled by their symmetry. For each symmetry sector $\alpha \in 0 \dots N-1$, let λ_α be the largest eigenvalue, with corresponding eigenvector r_α . That is $\mathbb{T}(r_\alpha) = \lambda_\alpha r_\alpha$ and

$$U r_\alpha U^\dagger = \omega^\alpha r_\alpha, \quad (4)$$

with $\omega = \exp(\frac{2\pi i}{N})$. Clearly r_α is not positive for any $\alpha \neq 0$, it is not even Hermitian unless $\omega^\alpha \in \mathbb{R}$ since then r_α^\dagger transforms according to the irrep $(\omega^\alpha)^* \neq \omega^\alpha$ (star denotes complex conjugation). From complete positivity of \mathbb{T} , its eigenvector corresponding to the largest eigenvalue should be positive and hence $|\lambda_0| \geq |\lambda_\alpha|$. We will assume that the eigenvalue λ_α is non-degenerate for each symmetry sector and that $|\lambda_0| > |\lambda_\alpha|$ unless an onset of an order parameter enforces them to be equal. Non-degeneracy in the trivial symmetry sector implies, by positivity of \mathbb{T} and r_0 , that $\lambda_0 > 0$. The PEPS tensors can be rescaled as $A \rightarrow \lambda_0^{\frac{1}{2N_v}} A$ to ensure that $\lambda_0 = 1$, making r_0 a fixed point of the transfer operator. We will refer to any eigenvector having eigenvalue 1 as fixed point, and their span as the fixed point space, of \mathbb{T} .

From Eq. (2) it is also clear that order parameters $\langle Z \rangle$ (with $uZ = \gamma Z u$, $\gamma \neq 1$) vanish by symmetry if the boundary tensors l and r are symmetric ($[l, S] = [r, S] =$

0). Also, for large d_3 , $\mathbb{T}^{d_3}(r)$ will converge to an eigenvector of \mathbb{T} with largest eigenvalue and having overlap with r . Similarly for $[\mathbb{T}^*]^{d_1}(l)$, where \mathbb{T}^* is the dual transfer operator: $\mathbb{T}^*(\rho) := \sum_i (B^i)^\dagger \rho B^i$. This suggests that, in the thermodynamic limit, symmetry breaking occurs if there exist a largest eigenvector of the transfer operator which is not symmetric. In the following section we will elaborate on this statement.

III. LONG RANGE ORDER IN THE TRANSFER OPERATOR

Given a local Hamiltonian H_0 with a symmetry $[H, u] = 0$, there are two ways to define symmetry breaking: The first is a non-vanishing spontaneous magnetization

$$m := \lim_{B \rightarrow 0} \lim_{\Lambda \rightarrow \infty} \frac{1}{N} \langle O \rangle_{B, \Lambda}, \quad (5)$$

and the other one a non-zero long-range order

$$\sigma := \lim_{\Lambda \rightarrow \infty} \frac{1}{N} \sqrt{\langle O^\dagger O \rangle_{0, \Lambda}}, \quad (6)$$

for some suitably chosen magnetization operator $O = \sum_{i \in \Lambda} Z_i$ (with local operators Z_i). Here, Λ refers to the set of all sites, and $\langle \cdot \rangle_{B, \Lambda}$ denotes the expectation value in the ground state of the Hamiltonian with a symmetry breaking field, $H_\Lambda(B) = H_0 + B \sum_{i \in \Lambda} Z_i$. It has been shown in a number of cases that $m \geq \sigma$, i.e., long-range order implies a non-zero spontaneous magnetization [2, 13]. It is for this reason that we consider PEPS wavefunctions with long-range order (which we will use interchangeably with symmetry breaking in the following); our goal will be on the one hand to understand the conditions under which long-range order occurs, and on the other hand to identify the wavefunctions describing the corresponding symmetry broken states (i.e., those obtained as ground states of $H_\Lambda(B)$ in the limit $B \rightarrow 0$).

Specifically, in the case of a \mathbb{Z}_N symmetry considered in this work, long-range order will denote a non-zero σ for some Z obeying

$$u^\dagger Z u = \omega^\alpha Z, \quad (7)$$

for some $\alpha = 0 \dots N-1$ and again $\omega = \exp(\frac{2\pi i}{N})$. The $\alpha = 1$ case we will refer to as full symmetry breaking since Z does not commute with any symmetry operation u^n . On the other hand, if $\text{gcd}(\alpha, N) > 1$, then the symmetry is only partially broken since Z commutes with $u^{N/\text{gcd}(\alpha, N)}$. The advantage of long range order as opposed to a non-zero order parameter for the detection of symmetry breaking is that a symmetric state can have long range order whereas any non-symmetric operator has zero expectation value with respect to a symmetric state. Evaluating m will require a symmetry breaking field and hence a non symmetric PEPS, which would not help us in understanding how a symmetric PEPS could

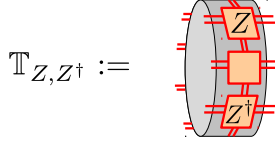


FIG. 3. The transfer operator $\mathbb{T}_{Z,Z^\dagger}^{[i,j]}$ dressed on two physical sites, where the full operator is given by all permutations

describe ordered phases. Evaluating σ can be done using a symmetric PEPS: we will even do so on a closed manifold (periodic boundary conditions) such that the full state is symmetric, as discussed in the previous section.

Let us now turn towards PEPS. For a PEPS $|\Psi\rangle$, we have that $\sigma^2 = \lim_{N_h, N_v \rightarrow \infty} \sigma_{N_v, N_h}^2$ where

$$\sigma_{N_v, N_h}^2 = \frac{1}{N_h^2 N_v^2} \sum_{ij} \frac{\langle \Psi | Z_i Z_j^\dagger | \Psi \rangle}{\langle \Psi | \Psi \rangle}. \quad (8)$$

In what follows, we will normalize Z_i such that its operator norm $\|Z_i\|_{\text{op}} \leq 1$. We will decompose the above sum over i and j into two parts: either $i_y \neq j_y$ or $i_y = j_y$. For the first part, define $\mathbb{T}_Z := \frac{1}{N_v} \sum_{k=1}^{N_v} \mathbb{T}_Z^{[k]}$ and for the second part define $\mathbb{T}_{Z,Z^\dagger} := \frac{1}{N_v^2} \sum_{i,j=1}^{N_v} \mathbb{T}_{Z,Z^\dagger}^{[i,j]}$ where $\mathbb{T}_{Z,Z^\dagger}^{[i,j]}$ is the transfer operator obtained by inserting an operator Z and Z^\dagger at sites i and j respectively, see Fig. 3.

Define C_1 and C_2 as

$$C_1 = \sum_{p=0}^{N_h-2} \text{Tr} [\mathbb{T}_{Z^\dagger} \mathbb{T}^p \mathbb{T}_Z \mathbb{T}^{N_h-p-2}] , \quad (9)$$

$$C_2 = \text{Tr} [\mathbb{T}_{Z,Z^\dagger} \mathbb{T}^{N_h-1}] . \quad (10)$$

This allows us to write $\sigma_{N_v, N_h}^2 = \frac{1}{N_h} \frac{C_1 + C_2}{\text{Tr}[\mathbb{T}^{N_h}]}$. The factors of N_v are taken care of by the definition of \mathbb{T}_{Z,Z^\dagger} and \mathbb{T}_Z and a factor of N_h is taken care of by using translation invariance in the horizontal direction. The contribution of C_2 converges to zero in the large N_h limit. It corresponds to taking the sum over $N_v^2 N_h$ expectation values and dividing by $N_v^2 N_h^2$. The term of interest is C_1 .

From the scaling of $\frac{C_1}{N_h \text{Tr}[\mathbb{T}^{N_h}]} \propto \mathcal{O}(1)$ we aim to show that the gap between $|\lambda_\alpha|$ and the largest eigenvalue λ_0 decreases with increasing N_h . A first step in the proof is that for large N_h , $\mathbb{T}^{N_h} \rightarrow |r_0\rangle\langle l_0|$, where r_0 is the eigenvector of \mathbb{T} corresponding to the eigenvalue λ_0 and l_0 the corresponding left eigenvector (ie. eigenvector of \mathbb{T}^*). We use round brackets to emphasize that, although r_0 and l_0 are eigenvectors, they are also operators. The dressed transfer operator \mathbb{T}_Z maps r_0 into the symmetry sector $\alpha = 1$ due to

$$\begin{aligned} U \mathbb{T}_Z(r_0) U^\dagger &= \mathbb{T}_{u^\dagger z_u}(U r_0 U^\dagger) \\ &= \omega \mathbb{T}_Z(r_0) . \end{aligned} \quad (11)$$

More explicitly, if $U U^\dagger = \omega^\beta l$, then $\text{Tr} [l^\dagger \mathbb{T}_Z(r_0)] \neq 0$ only if $\beta = \alpha$. The main idea is that the factor \mathbb{T}^p will

give rise to an exponential suppression, the leading term being proportional to $|\lambda_\alpha|^p$. So $|\lambda_\alpha| < 1$ will result in zero long range order. However, as N_v increases, the dimension of the space on which \mathbb{T} acts also increases exponentially as D^{2N_v} , where D is the bond dimension of the PEPS tensor A . Without any other assumptions, large Jordan blocks could prevent exponential suppression. As an example, consider a map T in Jordan form with a single Jordan block of size D and corresponding eigenvalue $\lambda < 1$. Then for $v = (0, \dots, 0, 1)^T$, $\|T^p v\|^2 = \sum_{q=0}^{\min(p,D)} \lambda^{2(p-q)} \binom{p}{q}^2$. For large p this sum scales as $\lambda^{2p} p^{2D}$, which for constant D is eventually exponentially suppressed but only at a length scale $p \propto D$. Hence, due to the exponentially increasing dimension of \mathbb{T} , correlations are only suppressed only over a length D^{2N_v} leading to a scaling of the long range order as $\sigma^2 \propto \frac{1}{N_h} D^{2N_h}$, even in the case that $|\lambda_\alpha| < 1$. It is for this reason that we need more assumptions on \mathbb{T} .

We will assume for the rest of the section that the transfer operator \mathbb{T} is normal, $\mathbb{T} \mathbb{T}^* = \mathbb{T}^* \mathbb{T}$. This is in particular the case if \mathbb{T} is Hermitian, which for example can follow from Hermiticity of its Kraus operators $(B^i)^\dagger = B^i$ which physically is related to a combination of time reversal (complex conjugation) and reflection along the y -axis (transposition) symmetry.

Let us now return to Eq. (9). In [12] it was shown that if the largest eigenvalue $\lambda_0 = 1$ of \mathbb{T} is non degenerate, then for any bounded operator O the following holds:

$$\begin{aligned} \lim_{N_h \rightarrow \infty} \sum_{p=0}^{N_h-2} \frac{\text{Tr} [\mathbb{T}_{O^\dagger} \mathbb{T}^p \mathbb{T}_O \mathbb{T}^{N_h-p-2}]}{\text{Tr} [\mathbb{T}^{N_h}]} &= \\ 2 \sum_{p=0}^{\infty} \text{Tr} [\mathbb{T}_{O^\dagger} \mathbb{T}^p \mathbb{T}_O |r_0\rangle\langle l_0|] &. \end{aligned} \quad (12)$$

The factor of two arises from first splitting the sum into two parts, one for which $p > N_h/2$ and one for which $p < N_h/2$. Both sums are identical (if N_h is odd) up to the position of the dagger, which can be swapped using ket-bra-hermiticity which exchanges $\mathbb{T}_O \leftrightarrow \mathbb{T}_O^\dagger$, while leaving the other terms unchanged, and thus $\sum_{p=0}^{N_h-2} \rightarrow 2 \sum_{p=0}^{N_h/2-1}$. (The original proof does not carry the dagger, but this can be easily adapted.)

Using Eq. (12), we now have that

$$\begin{aligned} \lim_{N_h \rightarrow \infty} N_h \sigma_{N_v, N_h}^2 &= \sum_{p=0}^{\infty} \text{Tr} [\mathbb{T}_{Z^\dagger} \mathbb{T}^p \mathbb{T}_Z |r_0\rangle\langle l_0|] \\ &= \sum_{p=0}^{\infty} \langle l_0 | \mathbb{T}_{Z^\dagger} (P_\alpha \mathbb{T}^p P_\alpha) |r_0\rangle \\ &\stackrel{(a)}{=} \langle l_0 | \mathbb{T}_{Z^\dagger} (1 - P_\alpha \mathbb{T} P_\alpha)^{-1} \mathbb{T}_Z |r_0\rangle \\ &\stackrel{(b)}{\leq} \| \langle l_0 | \mathbb{T}_{Z^\dagger} \|_2 \| (1 - P_\alpha \mathbb{T} P_\alpha)^{-1} \|_{\text{op}} \| \mathbb{T}_Z |r_0\rangle \|_2 \\ &\leq \frac{1}{1 - |\lambda_\alpha|} , \end{aligned}$$

where P_α is the projector onto the irrep sector α . It is in (a) and (b) that we have used normality of \mathbb{T} , which implies that $\|P_\alpha \mathbb{T} P_\alpha\|_{\text{op}} < 1$ such that the Neumann series converges, and $\|\mathbb{T}_Z |r_0\rangle\|_2^2 = \langle r_0 | \mathbb{T}_Z \mathbb{T}_Z |r_0\rangle \leq 1$, as $\|Z_i\|_{\text{op}} \leq 1$ and the left and right eigenvectors coincide.

We now have

$$\sigma^2 = \lim_{N_h, N_v \rightarrow \infty} \sigma_{N_v, N_h}^2 \leq \lim_{N_v \rightarrow \infty} \frac{1}{N_v} \lim_{N_h \rightarrow \infty} N_h \sigma_{N_v, N_h}^2, \quad (13)$$

where the inequality can be shown by coupling the l.h.s. limit such that N_h grows sufficiently faster than N_v , based on the formal definition of the limit [14]. It thus follows that if $\sigma^2 > 0$, for sufficiently large N_v it must hold that

$$0 < \frac{1}{N_v} \frac{1}{1 - |\lambda_\alpha|}. \quad (14)$$

Thus non zero long range order of an order parameter Z obeying Eq. (7) for some α implies that $|\lambda_\alpha| \geq 1 - \mathcal{O}(1/N_v)$.

At this point we have not said anything about the phase of λ_α . It is known that peripheral spectrum (eigenvalues of modulus 1) consists of roots of unity [15, Proposition 3.3] and that any eigenvalue of the form $e^{2\pi i/p}$ corresponds to a p periodic state. The degeneracy of the fixed point would then relate to a breaking of translation symmetry, as well as the global symmetry s . An example is the antiferromagnetic phase. We can remove such a phase by blocking p sites, i.e. consider \mathbb{T}^p , yielding that $\lambda_\alpha \geq 1 - \mathcal{O}(1/N_v)$.

IV. BOUNDARY OF GROUND STATES

Ground states in an ordered phase are not only eigenstates of a symmetric Hamiltonian, but also eigenstates of any perturbed Hamiltonian. Similarly, we will discuss in this section, which fixed points of the transfer operator are also fixed points of any perturbed transfer operator. In more detail, let $H = \sum_R h_R$ be the parent Hamiltonian of some PEPS defined by the tensors $A^{[i]}$. Consider the perturbation in which each local term is conjugated by an operator of the form $\Lambda_R = \Lambda^{\otimes |R|}$ where Λ is close to unity. The perturbed Hamiltonian

$$H_\Lambda = \sum_R (\Lambda^{-1})_R^\dagger h_R \Lambda_R^{-1}, \quad (15)$$

is clearly positive and annihilates the perturbed PEPS $|\Psi_\Lambda\rangle$ constructed from perturbed tensors $A_\Lambda^i := \sum_j \Lambda_{ij} A^j$. Hence $|\Psi_\Lambda\rangle$ is the ground state of H_Λ . We will restrict ourselves to perturbing tensors as $\sum_j \Lambda_{ij} A^j$, keeping in mind that the corresponding PEPS is a ground state of a perturbed Hamiltonian. The fixed points of \mathbb{T} , which are also fixed points of any perturbed transfer matrix \mathbb{T}_Λ , correspond to the boundary of those eigenstates of the parent Hamiltonian, which are also eigenstates of

any perturbed parent Hamiltonian, of the form given in Eq. (15). In other words, fixed points of \mathbb{T} stable under any perturbation arising from Λ describe the boundary of ground states. We will refer to them as *stable* fixed points. Concretely, a set of stable fixed points satisfies:

$$\mathbb{T}_\infty \mathbb{T}_\Lambda R_i \propto R_i \quad \forall \quad \Lambda, \quad (16)$$

where \mathbb{T}_∞ is the projector onto the fixed point space.

In the following, we will determine the structure of this fixed point space. We start in Sec. IV 1 by showing that any set $\{R_i\}_i$ spanning the fixed point space is stable under perturbations if the R_i are all positive and mutually orthogonal. We then continue in Sec. IV 3 by showing how to explicitly construct such a set of stable fixed points for the case where the transfer operator is unital and has a full rank left positive fixed points. (Section IV 2 discusses technical result by Wolf [16] needed for the proof, showing that the fixed point space of a unital channel, having a full rank left fixed point, forms an algebra.) Finally, we show in Sec. IV 4 that a set of stable fixed points can be explicitly constructed in the same way even if these conditions are not met.

1. Conditions for stability

Let us first consider the case where we are given a basis $\{R_i\}_i$ of the fixed point space which satisfies that the R_i are all positive and moreover mutually orthogonal: $\text{Tr}(R_i R_j) = 0$ for $i \neq j$. We will show that under these conditions, the fixed point space is stable, i.e., Eq. (16) holds.

Let $\{L_i\}_i$ be a basis of the fixed point space of the dual transfer operator \mathbb{T}^* , which is dual to $\{R_i\}_i$ in the sense that $\text{Tr}(L_i^\dagger R_j) = \delta_{ij}$. We can use them to write the projector onto the fixed point space $\mathbb{T}_\infty(\rho) = \sum_i R_i \text{Tr}(L_i^\dagger \rho)$ and its dual map $\mathbb{T}_\infty^*(\rho) = \sum_i L_i \text{Tr}(R_i^\dagger \rho)$. Since \mathbb{T}_∞ is completely positive we have that $\mathbb{T}_\infty^*(R_j) = \sum_i L_i \text{Tr}(R_i^\dagger R_j) = L_j$ is positive. Here we use positivity and orthogonality of R_i . In order to prove Eq. (16) it is sufficient to show that $\text{tr}[L_i \mathbb{T}_\Lambda(R_j)] = 0$ if $i \neq j$. Let $M_{ij} = \sum_{\alpha\delta k} \sum_{\beta\gamma} \sqrt{L_{i\alpha\beta}} B_{\beta\gamma}^k \sqrt{R_{j\gamma\delta}} |\alpha k \delta\rangle$. Using positivity of both L_i and R_j we obtain the following equation:

$$\text{Tr}[L_i \mathbb{T}_\Lambda(R_j)] = \langle M_{ij} | \mathbb{I} \otimes \Lambda \otimes \mathbb{I} | M_{ij} \rangle \quad \forall i, j. \quad (17)$$

Also, by construction of M_{ij} we have that $\langle M_{ij} | M_{ij} \rangle = \text{tr}[L_i \mathbb{T}(R_j)] = \delta_{ij}$. Combining these facts we conclude that indeed that indeed $\text{tr}[L_i \mathbb{T}_\Lambda(R_j)] = 0$ if $i \neq j$ and hence that the set of $\{R_i\}_i$ is a stable set of fixed points.

2. Structure of the fixed point space

Following [16], we will show that the fixed point set of unital transfer operators, whose dual has a positive full

rank fixed point, is an algebra. The algebra structure will allow us to construct a set of positive, i.e., stable fixed points in the following subsection. Starting point is a Cauchy-Schwarz like inequality for unital CP maps \mathbb{T} [16]:

$$\mathbb{T}(AA^\dagger) \geq \mathbb{T}(A)\mathbb{T}(A^\dagger). \quad (18)$$

This can be verified by taking the Stinespring representation $\mathbb{T}(A) = V(A \otimes \mathbb{I})V^\dagger$ with V an isometry, i.e. $V^\dagger V \leq \mathbb{I}$. Let R be a fixed point of the unital CP map \mathbb{T} and L a fixed point of the dual map \mathbb{T}^* and consider the equality $\text{tr}[L(\mathbb{T}(RR^\dagger) - \mathbb{T}(R)\mathbb{T}(R^\dagger))] = \text{tr}[\mathbb{T}^*(L)RR^\dagger - LRR^\dagger] = 0$, where we have used $\mathbb{T}(R) = R$ and $\mathbb{T}^*(L) = L$. From Eq. (18) it already follows that $\mathbb{T}(RR^\dagger) - \mathbb{T}(R)\mathbb{T}(R^\dagger)$ is positive. Hence if L is positive and has full rank, this equality tells us that

$$\mathbb{T}(RR^\dagger) = \mathbb{T}(R)\mathbb{T}(R^\dagger). \quad (19)$$

Now, in order to show that the fixed point space of \mathbb{T} is an algebra, take two fixed points R_1 and R_2 and apply Eq. (19) to $R = R_1 + t^*R_2^\dagger$ for some complex t :

$$\begin{aligned} 0 &= \mathbb{T}(R_1 R_1^\dagger) - \mathbb{T}(R_1)\mathbb{T}(R_1^\dagger) \\ &+ t[\mathbb{T}(R_1 R_2) - \mathbb{T}(R_1)\mathbb{T}(R_2)] \\ &+ t^*[\mathbb{T}(R_2^\dagger R_1^\dagger) - \mathbb{T}(R_2^\dagger)\mathbb{T}(R_1^\dagger)] \\ &+ |t|^2[\mathbb{T}(R_2^\dagger R_2) - \mathbb{T}(R_2^\dagger)\mathbb{T}(R_2)]. \end{aligned} \quad (20)$$

The terms constant and quadratic in t vanish due to Eq. (19). By replacing $t \rightarrow it$, adding the two equalities, one ends up with $\mathbb{T}(R_1 R_2) = \mathbb{T}(R_1)\mathbb{T}(R_2)$

3. Construction of stable fixed points

Let us now show how the algebra structure can be used to construct positive orthogonal right fixed points for unital channels. In the following subsection, we will then show how to adapt these arguments for the case of non-unital channels.

In the presence of long range order, there is a fixed point r_α for each symmetry sector α . Due to the non-degeneracy of fixed points per symmetry sector we have that $r_\alpha r_\beta \propto r_{\alpha+\beta}$. The algebra of fixed points of \mathbb{T} is hence generated by a single element, in the case of full symmetry breaking being r_1 , which we can choose to normalize to $r_1^N = \mathbb{I}$. We can set all other fixed points such that $r_\alpha := r_1^\alpha$. We also have, using non-degeneracy again, that $r_1^\dagger = \gamma r_1^{-1}$. Taking the N -th power of this equation shows that γ is an N -th root of unity. Multiplying this equation with r_1 shows that γ should be positive. Hence $\gamma = 1$ and r_1 and thus also r_α , is unitary for all α .

The rich structure of the fixed point space of \mathbb{T} allows us to define the following orthogonal projectors:

$$R_i = \frac{1}{N} \sum_\alpha \omega^{i\alpha} r_\alpha. \quad (21)$$

From $r_\alpha r_\beta = r_{\alpha+\beta}$ it follows that $R_i R_j = \delta_{ij} R_i$ and from $r_\alpha^\dagger = r_{N-\alpha}$ it follows that $R_i^\dagger = R_i$. Hence these fixed points are both orthogonal and positive.

4. Generalization to non-unital transfer operators

The transfer operators we are considering are not necessarily unital. The general idea to fix this is to replace \mathbb{T} by $\tilde{\mathbb{T}} : \rho \mapsto \sqrt{r_0^{-1}} \mathbb{T}(\sqrt{r_0} \rho \sqrt{r_0}) \sqrt{r_0^{-1}}$, which is again unital, where r_0 is a positive and full-rank right fixed point. To also cover the general case where r_0 is not full rank, we consider that there exist two maps V and W satisfying $[W^\dagger V, U] = 0$, $VW^\dagger = \mathbb{I}$ and

$$\text{Tr}(Wl^\dagger W^\dagger V r V^\dagger) = \text{Tr}(l^\dagger r), \quad (22)$$

for any pair of left and right fixed point l and r of \mathbb{T} , where $V r_0 V^\dagger = \mathbb{I}$ and $W l_0 W^\dagger$ is positive full rank for some right and left fixed point r_0 and l_0 with irrep $\alpha = 0$, respectively. In the Appendix, we show how to explicitly construct such V and W in the general case; for the generic case where \mathbb{T} already has a full rank positive left and right fixed point, we can choose $V = \sqrt{r_0}$ and $W = \sqrt{r_0^{-1}}$.

Let us again denote the unique fixed points of \mathbb{T} in each irrep sector α by r_α and l_α , respectively. We now introduce a modified transfer operator $\tilde{\mathbb{T}} = V \mathbb{T}_\infty (W^\dagger \rho W) V^\dagger$ where again \mathbb{T}_∞ is the projector onto the fixed point space of \mathbb{T} . We have that $\tilde{\mathbb{T}}(\rho) = \sum_i \tilde{r}_\alpha \text{Tr}(\tilde{l}_\alpha^\dagger \rho)$, where $\tilde{r}_\alpha := V r_\alpha V^\dagger$ and $\tilde{l}_\alpha := W l_\alpha W^\dagger$. Since $\text{Tr}[\tilde{l}_\alpha^\dagger \tilde{r}_\beta] = \text{Tr}[l_i^\dagger r_j] = \delta_{ij}$ (implied by Eq. (22)) it follows that the \tilde{r}_α are fixed points of $\tilde{\mathbb{T}}$, with dual fixed points \tilde{l}_α . Thus, $\tilde{\mathbb{T}}$ is unital (as $\tilde{r}_0 = \mathbb{I}$) and has a full rank positive left fixed point (namely \tilde{l}_0). In addition, $\tilde{\mathbb{T}}$ has the same \mathbb{Z}_N symmetry with generator $\tilde{U} = V U W^\dagger$, and the \tilde{r}_α and \tilde{l}_α transform accordingly. Therefore, we can apply the results of Sec. IV 3 to find the stable fixed points of $\tilde{\mathbb{T}}$, $\tilde{R}_i = \sum \omega^{i\alpha} \tilde{r}_\alpha$, as well as the corresponding

$$R_i = \sum \omega^{i\alpha} r_\alpha, \quad (23)$$

which by construction satisfy $\tilde{R}_i = V R_i V^\dagger$, and corresponding left fixed points $\tilde{L}_i = \sum \omega^{i\alpha} l_\alpha$, $\tilde{L}_i = W L_i W^\dagger$. Now consider a perturbation \mathbb{T}_Λ of \mathbb{T} . We have that

$$\text{Tr}[L_i^\dagger \mathbb{T}_\Lambda(R_j)] = \text{Tr}[L_i^\dagger \mathbb{T}_\infty \mathbb{T}_\Lambda \mathbb{T}_\infty(R_j)] = \text{Tr}[\tilde{L}_i^\dagger \tilde{\mathbb{T}}_\Lambda(\tilde{R}_j)],$$

where we defined $\tilde{\mathbb{T}}_\Lambda(\rho) := V \mathbb{T}_\infty \mathbb{T}_\Lambda \mathbb{T}_\infty (W^\dagger \rho W) V^\dagger$ and used (22). Since $\tilde{\mathbb{T}} = \tilde{\mathbb{T}}_1$, $\tilde{\mathbb{T}}_\Lambda$ is indeed a (special) perturbation of $\tilde{\mathbb{T}}$, and using the result of Sec. IV 1, we find that the r.h.s. and thus also $\text{Tr}[L_i^\dagger \mathbb{T}_\Lambda(R_j)] = 0$ unless $i = j$, proving the stability of the basis R_i, L_j against perturbations.

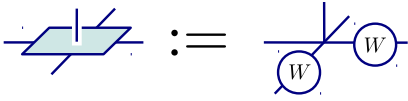


FIG. 4. The Potts PEPS tensor is defined as a dimension three (bond and physical) delta-tensor contracted with a matrix $M(\beta)$ (see text) on two adjacent virtual indices.

V. NUMERICAL STUDY: THE 3-STATE POTTS MODEL

In this section we numerically study symmetry breaking in a quantum model derived from the classical 3-state Potts model which has a \mathbb{Z}_3 symmetry. We find that in the ordered phase, corresponding to low temperatures, there is indeed a degeneracy in the largest eigenvalue of the transfer operator, which is not the case in the disordered phase. The corresponding fixed points can be labeled according to their symmetry. We compare these symmetric fixed points to the set of stable fixed points, which are also fixed points of a perturbed transfer matrix. First, we check that these are indeed related to each other by a Fourier transform, see Eq. (21). And secondly, we compare the locality of their corresponding boundary Hamiltonians.

The Hamiltonian of the 3 state Potts model is given by $H = -\sum_{\langle i,j \rangle} \delta(s_i, s_j)$, where s_i is a classical spin variable at site i taking values 0, 1 or 2. Its partition function $Z = \text{Tr} e^{-\tau H}$ at inverse temperature τ is equal to the norm squared of a (unnormalized) Rokhsar-Kivelson-type wave function: $|\Phi(\tau)\rangle := \sum_{\{s_i\}} e^{-\tau/2H(\{s_i\})} |\{s_i\}\rangle$. Indeed, the correlations of $|\Phi(\tau)\rangle$ in the diagonal basis are exactly the same as for the corresponding Potts model, and it thus exhibits a phase transition at the very same value of τ . This wave function has an exact PEPS description [10], cf. Fig. 4: the PEPS tensors, having bond dimension 3, are given by $A_{\alpha\beta\gamma\eta}^{s_i} = \sum_{\zeta\theta} \delta_{s_i=\alpha=\beta=\zeta=\theta} W(\tau)_{\zeta\gamma} W(\tau)_{\theta\eta}$. The matrices $W(\tau)$, sitting on the virtual links, take care of the contribution $e^{-\tau/2h(s_i, s_j)}$ of the spins s_i and s_j neighboring the corresponding virtual link. Up to normalization, it is given by

$$W(\tau) := \begin{pmatrix} 1 & a & a \\ a & 1 & a \\ a & a & 1 \end{pmatrix}, \quad (24)$$

where $a = e^{-\tau/2}$. We use the parameter $\theta \in [0, 1]$, related to inverse temperature τ as $e^{-\tau/2} = \sin(\pi\theta/2)$ to interpolate between the ordered and the disordered phases. In terms of this parameter, the phase transition takes place at $\theta_c \approx 0.4149$. The matrix W is invariant under a \mathbb{Z}_3 action, realized by a cyclic shift of the basis vectors, hence the full tensor $A_{\alpha\beta\gamma\delta}^{s_i}$ has a symmetry in the sense

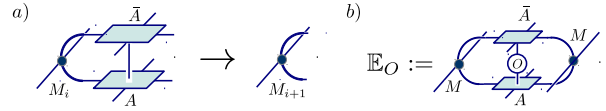


FIG. 5. iMPS method, cf. text. (a) Iteration step $\mathbb{T}M_i \rightarrow M_{i+1}$. (b) The operator \mathbb{E}_O used to compute correlation length and order parameter.

of Eq. (1) with

$$s = S = \begin{pmatrix} 0 & 1 & 0 \\ 0 & 0 & 1 \\ 1 & 0 & 0 \end{pmatrix}. \quad (25)$$

1. Phase transition

In figure Fig. 6(a) we report on the spectral gap between the largest and second largest eigenvalue of the transfer operator. These values are obtained by exact diagonalization of a transfer operators of a different sizes N_v (6, 8 or 10). We clearly observe a degeneracy in the ordered phase and a non-zero gap in the disorderd phase. The transition becomes sharper as we increase N_v , ie. when finite size effects are decreased.

Additionally, to verify the critical value θ_c , we use an infinite Matrix Product State (“iMPS”) algorithm to determine correlation lengths and magnetization. The iMPS algorithm produces a translational invariant MPS description of the fixed point of a transfer operator for which $N_v \rightarrow \infty$, thereby avoiding any finite size effects. Inspired by the fact that \mathbb{T}^∞ projects onto the fixed point space, such algorithms start off with an arbitrary translational invariant MPS M , from which a sequence of MPSS are created recursively by application of the transfer operator: $\mathbb{T}M_i \rightarrow M_{i+1}$. Crucially, at each step truncation takes place to keep the bond dimension from growing. This is done by truncating the singular values of $\sqrt{L}\sqrt{R}$, where L and R are the left and right largest eigenvector of the transfer matrix \mathbb{E} of the MPS.

The fixed points of the transfer operator can be used to efficiently contract a tensor network representing the expectation values of local operators. As a result, such values can be written purely in terms of the MPS tensor M of the fixed point. Let $\mathbb{E}_O = \sum_i M^i \otimes B_O \otimes \bar{M}^i$ be the dressed transfer matrix corresponding to the fixed point MPS [17]. The correlation length is related to the spectral gap of $\mathbb{E}_\mathbb{I}$ as $\xi = -(\log \frac{\lambda_1}{\lambda_0})^{-1}$, where λ_i is the i -th eigenvector of $\mathbb{E}_\mathbb{I}$. The expectation value of a local operator is given by $1/\lambda_0 \langle l | \mathbb{E}_O | r \rangle$, where r and l are the right and left eigenvectors of $\mathbb{E}_\mathbb{I}$, respectively. We calculate the correlation length, Fig. 6(b), and the the expectation value of $Z = \text{diag}(1, \omega, \bar{\omega})$, which acts as an order parameter since it does not commute with the symmetry u , Fig. 6(c). The data shows a diverging correlation length,

together with the onset of the order parameter, at the expected value of transition. Moreover, we take confidence from here, that a moderate bond dimension is sufficient to describe the fixed point, away from the critical point, since the correlation length saturates with increasing χ .

Note that from the onset of an order parameter we can conclude that we have obtained a symmetry broken fixed point from the iMPS algorithm, even though we have not explicitly broken the symmetry of the transfer operator. Indeed, it is well-known that variational methods tend to spontaneously break symmetries since they generally prefer states with fewer long-range correlations. It is however not clear a priori whether this symmetry breaking is the same as the one derived in the Section IV using *physical* perturbations of the transfer operator, although it is plausible to assume that the numerical inaccuracies giving rise to the observed symmetry breaking act in an equivalent way.

2. Stability of fixed points

We continue by explicitly verifying the relation between stable fixed points and symmetric fixed points in the ordered phase. For finite N_v , exact diagonalization easily allows to extract the symmetric fixed points by using projectors on the different symmetry sectors. Note that the symmetric fixed points are defined up to a phase. We set this phase by insisting that the largest eigenvalues of the fixed points be positive. The stable fixed points are obtained by explicitly breaking the symmetry of the PEPS tensor (and hence of the transfer operator) by $A \rightarrow (\mathbb{I} + \epsilon Z)A$ where again $Z = \text{diag}(1, \omega, \bar{\omega})$.

In Fig. 6(d) we report on the infidelity per site $\delta = \min_i(1 - \langle R_i | R_\epsilon \rangle) / N_v$ between the stable fixed points R_ϵ and the Fourier transform of the symmetric fixed points R_i given by Eq. (4) at $\theta = 0.25 < \theta_c$ (well into the ordered phase). We observe infidelities of the order of $10^{-5} - 10^{-10}$ and thus conclude that the stable fixed points are indeed well approximated by the Fourier transform of symmetric fixed points. We further observe that the infidelity per site scales as ϵ^2 and is independent of system size N_v . This can be understood from perturbation theory. Up to quadratic terms in ϵ , the perturbed transfer operator is given by $\mathbb{T} + \epsilon \sum_{k=1}^{N_v} \mathbb{T}_{Z+Z^\dagger}^{[k]}$. The perturbed fixed point is given by $R_\epsilon \approx \frac{1}{\sqrt{1 + \epsilon^2 \text{Tr}(R_i^{\dagger 2})}} (R_i + \epsilon R_i^\perp)$ where R_i^\perp is orthogonal to R_i . This explains the ϵ dependency of the infidelity. Moreover $R_i^\perp = \sum_{k=1}^{N_v} \sum_n \frac{V_{n0}^{[k]}}{1 - \lambda_n} \rho_n$ where $V_{n0}^{[k]}$ is the coupling between the fixed point R_i and eigenstate ρ_n (with eigenvalue $\lambda_n < 1$) due to the perturbation $\mathbb{T}_{Z+Z^\dagger}^{[k]}$. The fact that $|R_i^\perp|^2$ scales linearly with N_v is consistent with R_i being finitely correlated: $V_{n0}^{[k]}$ only couples to states ρ_n which differ from R_i in a neighborhood of site k .

The above analysis breaks down as soon as the perturbation ϵ is weaker than the coupling between the stable

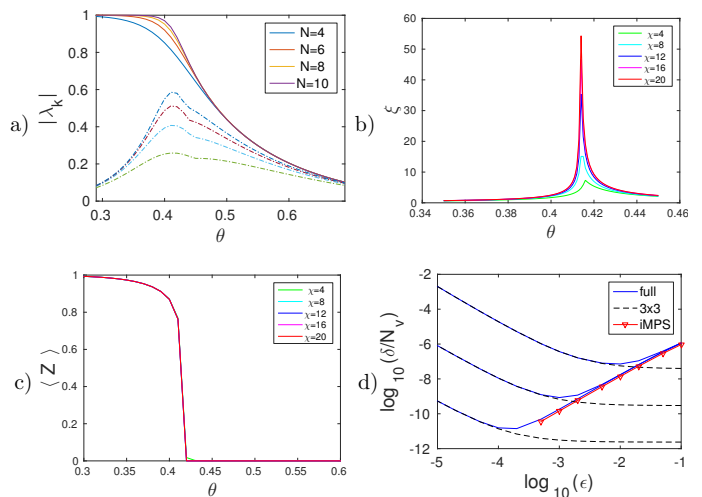


FIG. 6. 3-state Potts PEPS model a) Second- and fourth-largest eigenvalue of the transfer operator for finite size (second and third are (numerically) exactly degenerate) b) correlation length of the fixed point iMPS for increasing iMPS bond dimension χ c) order parameter $\langle Z \rangle$ measured on iMPS fixed point d) perturbation strength against infidelity per site for perturbation scaling analysis. blue: exact diagonalization on $N_v = 10$ (compressed), red: iMPS, dashed: exact diagonalization ($N_v = 10$) on $\{r_0, r_\omega, r_{\bar{\omega}}\}$ subspace ($\theta = 0.25$)

fixed points due to finite size effects. This explains the increase in infidelity below a certain ϵ_t . As expected, the value of ϵ_t decreases with increasing size. To further analyze this effect, we have also considered the restriction of the perturbed transfer operator \mathbb{T}_ϵ to the 3 dimensional fixed point space of \mathbb{T} , i.e. the space spanned by r_α [18]. Finding the fixed points of $\mathbb{I}\mathbb{T}_\epsilon\mathbb{I}$ (where \mathbb{I} is the orthogonal projection onto the fixed point space of \mathbb{T}) amounts to simply diagonalizing a 3 by 3 matrix of the form $T(\epsilon) = \mathbb{I} + \Delta + \epsilon P$. Here Δ is the finite size effect and is hence diagonal in the symmetric fixed point basis, and P is the perturbation. Again we report on infidelity $\delta = \min_i(1 - \langle R_i | R_\epsilon \rangle) / N_v$ with R_ϵ the fixed point of $\mathbb{I}\mathbb{T}_\epsilon\mathbb{I}$ and R_i again the Fourier transform of the symmetric fixed point of the unperturbed transfer operator, see Fig. 6(d). For small ϵ this infidelity is completely identical to earlier obtained infidelities at same system sizes. Thus the competition between splitting due to finite size effects and perturbation completely explains the observed infidelities. Interestingly, for large ϵ the fidelity saturates. In this regime, eigenstates of $T(\epsilon)$ are simply eigenstates of P but are apparently not exactly equal to the Fourier transform of the symmetric fixed points, as we would have expected from the discussion in Section IV. Note that, in proving that the stable fixed points are of the form $R_i = \sum_\alpha \omega^{i\alpha} r_\alpha$ we assumed an exact degeneracy, any finite size splitting could hence also alter the relation between the stable and the symmetric fixed points.

To avoid finite size effects, we also calculate the fixed point of the transfer operator with $N_v \rightarrow \infty$ using the

iMPS method. In this case, we do not verify Eq. (21) explicitly but rather verify that the obtained fixed point has large overlap with the stable fixed point. Overlaps between MPSs $|\phi_M\rangle$ and $|\phi_N\rangle$ are given by $\left(\frac{\lambda_{MN}^2}{\lambda_{MM}\lambda_{NN}}\right)^N$ where λ_{MN} is the largest eigenvalue of the mixed transfer matrix $\mathbb{E} = \sum_i M^i \otimes N^i$. Hence the infidelity per site, when it is small, is well approximated by $\delta = 1 - \frac{\lambda_{MN}^2}{\lambda_{MM}\lambda_{NN}}$. We find that the infidelity is again of the order of $10^{-5} - 10^{-10}$, see Fig. 6(d). Moreover, we find that it scales as ϵ^2 also for small ϵ .

3. Locality of fixed points

To further quantify the difference between stable and symmetric fixed point, we study the locality of their corresponding boundary Hamiltonian. The entanglement or boundary Hamiltonian is defined via its Gibbs state

$$\rho_A = \exp(-H_E) \Leftrightarrow H_E = -\log(\rho_A), \quad (26)$$

where ρ_A is a fixed point of the transfer operator. In the ordered phases it is a priori unclear which of the degenerate fixed points one should consider although Hermiticity of the Hamiltonian does imply positivity of the corresponding fixed point. Note that all stable fixed points and fixed points in the trivial symmetry sectors are positive. We report on the locality of the boundary Hamiltonian by decomposing it into k -local terms:

$$H = \sum_{i,k} h_i^{(k)} \Gamma_i^{(k)}, \quad \Gamma_i^{(k)} = \mathbb{I} \otimes \dots \otimes \mathbb{I} \otimes \underbrace{X \otimes \dots \otimes Y}_{k \text{ sites apart}} \otimes \mathbb{I} \otimes \dots \otimes \mathbb{I}. \quad (27)$$

The terms $\Gamma_i^{(k)}$ have non-trivial support on only k consecutive sites. Specifically, we construct $\Gamma_i^{(k)}$ by taking tensor products of Gell-Mann-matrices which constitute an orthonormal basis for 3×3 Hermitian matrices (under the Hilbert-Schmidt inner product). Let $w_k = \sum_i (h_i^{(k)})^2$ be the total strength of all k -local contributions. We report on w_k as a function of k for boundary Hamiltonians obtained at different temperatures. The fixed points used here are obtained by first using the iMPS algorithm to generate the MPS representation of a fixed point. We then use 8 copies of these matrices to approximate the fixed point of a transfer operator of size $N_v = 8$. This method allows use to study a finite size transfer operator whilst minimizing finite size effects.

In the disordered phase, the w_k decrease exponentially with k , indicating a *local* boundary Hamiltonian, see Fig. 7(a). The exponent increases as one approaches the phase transition. At the phase transition the weights w_k still seem to decay exponentially with k . Beyond the phase transition, we study both the locality of the fixed point obtained from iMPS (i.e. the stable fixed point) as well as a symmetrized version $r_0 = \sum_i U^i R U^{i\dagger}$. In Fig. 7(b) it can be seen that as we go away from phase

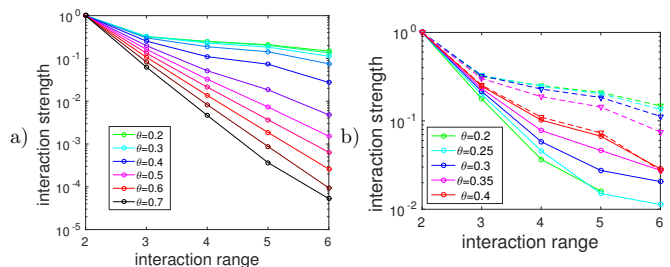


FIG. 7. Interaction strength (\log_{10}) vs. interaction range for the 3-state Potts model PEPS. Computed with iMPS and put on a cylinder of length 8. Fig. a) The weights of the symmetric fixed point clearly become non-local in the symmetry broken phase (since we get the symmetry broken fixed points with iMPS, we restore the symmetry with a twirl) b) Now in the symmetry broken phase $\theta < 0.41$ we compare the weights of the boundary Hamiltonians obtained from symmetric (dashed lines) and symmetry broken fixed points (solid lines), note that the color ordering matches, i.e. while the symmetry broken one gets more local, the symmetric one gets increasingly non-local.

transition, the locality of the symmetric fixed point increases whereas that of the stable fixed point decreases. Hence we find that the boundary Hamiltonian corresponding to the symmetric fixed point is less local than the boundary Hamiltonians corresponding to the stable fixed points, reinforcing the perspective that the symmetry broken fixed points are the ones which are physically relevant.

VI. CONCLUSIONS

In this work, we have studied the occurrence of symmetry breaking and long-range order in PEPS models with a \mathbb{Z}_N symmetry. Firstly, we have shown that long-range order is accompanied by a degeneracy in the spectrum of the transfer operator, with the gap closing at least as $1/N_v$. We have subsequently studied how the PEPS reacts to physical perturbations, i.e., those corresponding to perturbations of the Hamiltonian, and have determined the fixed points of the transfer operator (i.e., the boundary conditions to the system) which are stable under perturbations and thus describe the symmetry broken states. We have found that these states are uniquely determined by the symmetry structure of the transfer operator together with the requirement that they are positive, and are given by the Fourier transform of the fixed points in the individual symmetry sectors. We have finally numerically studied symmetry breaking in a PEPS model related to the \mathbb{Z}_3 Potts model, where we confirmed the relation between long-range order and the degeneracy of the transfer operator, as well as the form of symmetry broken fixed points. We subsequently computed the entanglement Hamiltonian both for the symmetric and the symmetry broken fixed points, and found that unlike the symmetric one, the symmetry broken fixed points give

rise to a quasi-local entanglement Hamiltonian, demonstrating the local nature of the entanglement Hamiltonian also for symmetry broken phases.

ACKNOWLEDGMENTS

We acknowledge helpful discussions with Mohsin Iqbal. This work has been supported by the Alexander von

Humboldt foundation, the European Union through the ERC grant WASCOSYS (No. 636201), and by JARA-HPC through grants jara0092 and jara0111.

-
- [1] R. B. Griffiths, Phys. Rev. **152**, 240 (1966).
 [2] T. Koma and H. Tasaki, Comm. Math. Phys. **158**, 191 (1993).
 [3] m. b. hastings, phys. rev. b **73**, 085115 (2006), cond-mat/0508554.
 [4] A. Molnar, N. Schuch, F. Verstraete, and J. I. Cirac, Phys. Rev. B **91**, 045138 (2015), arXiv:1406.2973.
 [5] F. Verstraete and J. I. Cirac, (2004), cond-mat/0407066.
 [6] R. Orus, Ann. Phys. **349**, 117 (2014), arXiv:1306.2164.
 [7] D. Perez-Garcia, F. Verstraete, J. I. Cirac, and M. M. Wolf, Quantum Inf. Comput. **8**, 0650 (2008), arXiv:0707.2260.
 [8] J. I. Cirac, D. Poilblanc, N. Schuch, and F. Verstraete, Phys. Rev. B **83**, 245134 (2011), arXiv:1103.3427.
 [9] S. Yang, L. Lehman, D. Poilblanc, K. V. Acoleyen, F. Verstraete, J. Cirac, and N. Schuch, Phys. Rev. Lett. **112**, 036402 (2014), arXiv:1309.4596.
 [10] F. Verstraete, M. M. Wolf, D. Perez-Garcia, and J. I. Cirac, Phys. Rev. Lett. **96**, 220601 (2006), quant-ph/0601075.
 [11] N. Schuch, D. Poilblanc, J. I. Cirac, and D. Perez-Garcia, Phys. Rev. Lett. **111**, 090501 (2013), arXiv:1210.5601.
 [12] M. Rispler, K. Duivenvoorden, and N. Schuch, Phys. Rev. B **92**, 155133 (2015), arXiv:1505.04217 [cond-mat.str-el].
 [13] T. Kaplan, P. Horsch, and W. von der Linden, Journal of the Physical Society of Japan **58**, 3894 (1989), <http://dx.doi.org/10.1143/JPSJ.58.3894>.
 [14] Let $\tau_{N_v} = \lim_{N_h} N_h \sigma_{N_h, N_v}^2$, and let $S := \lim_{N_v} \tau_{N_v}$. Then, for any $\epsilon > 0$,

$$\begin{aligned} \exists N_v^0 \forall N_v \geq N_v^0 : \left| \frac{1}{N_v} \tau_{N_v} - S \right| < \frac{\epsilon}{2} \quad \text{and} \\ \exists N_h^0(N_v) \forall N_h \geq N_h^0(N_v) : \frac{1}{N_v} \left| N_h \sigma_{N_h, N_v}^2 - \tau_{N_v} \right| < \frac{\epsilon}{2}. \end{aligned}$$

Thus,

$$\left| \frac{N_h}{N_v} \sigma_{N_h, N_v}^2 - S \right| \leq \epsilon,$$

and finally

$$\sigma^2 = \lim_{N_h, N_v \rightarrow \infty} \sigma_{N_h, N_v}^2 \leq \frac{N_h}{N_v} \sigma_{N_h, N_v}^2 = S,$$

as long as we couple the limits such that both $N_h \geq N_h^0(N_v)$ and $N_h \geq N_v$. (If $S = \infty$, the inequality (13) holds trivially.) Let us note that for normal \mathbb{T} , the convergence in Eq. (12), Ref. [12], yields a scaling $N_h^0(N_v) \propto N_v / (1 - |\lambda_\alpha(N_v)|)$, such that a non-zero σ^2 for all isotropically coupled limits $N_h/N_v = \text{const.}$ is sufficient to infer that $|\lambda_\alpha| \rightarrow 1$ as $N_v \rightarrow \infty$.

- [15] M. Fannes, B. Nachtergaele, and R. F. Werner, Comm. Math. Phys. **144**, 443 (1992).
 [16] M. M. Wolf, “Quantum Channels and Operations, Guided Tour,” (2012).
 [17] When left and right fixed points are described by different MPS M_L and M_R one should consider the mixed transfer matrix $\mathbb{E}_O = \sum_i M_L^i \otimes B_O \otimes M_R^i$.
 [18] Strictly speaking, due to finite size effects, these are not all fixed points.

Appendix: Construction of V and W

Consider a transfer operator (CP-map) \mathbb{T} with symmetry U as in Eq. (3). In this Appendix we will construct the V and W used in Sect. IV 4, i.e., which satisfy that there exist a left and right fixed point R_0 and L_0 of \mathbb{T} such that $VR_0V^\dagger = \mathbb{I}$ and WL_0W^\dagger is positive and full rank, $VW^\dagger = \mathbb{I}$, $[W^\dagger V, U] = 0$, and Eq. (22) holds for any pair of fixed points R and L of \mathbb{T} .

Let $R_0 = \mathbb{T}_\infty(\mathbb{I})$ and $L_0 = \mathbb{T}_\infty^*(\mathbb{I})$. Both R_0 and L_0 are positive due to positivity of \mathbb{T} and are symmetric due to Eq. (3). Let P_1 be the isometry ($P_1P_1^\dagger = \mathbb{I}$) such that $P_1^\dagger P_1$ projects onto the support of R_0 and let P_2 be isometry ($P_2P_2^\dagger = \mathbb{I}$) such that $P_2^\dagger P_2$ projects onto the support of $\hat{L}_0 = \sqrt{\hat{R}_0} P_1 L_0 P_1^\dagger \sqrt{\hat{R}_0}$, with $\hat{R}_0 := P_1 R_0 P_1^\dagger$. The maps V and W are given by:

$$V = P_2 \sqrt{\hat{R}_0^{-1}} P_1, \quad (\text{A.1})$$

$$W = P_2 \sqrt{\hat{R}_0} P_1. \quad (\text{A.2})$$

Note that \hat{R}_0 is by construction invertible. It can be straightforwardly checked that $VR_0V^\dagger = \mathbb{I}$. By definition of P_2 , WL_0W^\dagger is full rank. It is also positive since L_0 is positive. Also it is obvious that $VW^\dagger = \mathbb{I}$. It remains to check that $[W^\dagger V, U] = 0$ and Eq. (22) holds for any pair of fixed points R and L of \mathbb{T} .

The symmetry condition follows from the symmetry of R_0 and L_0 . From $[R_0, U] = 0$ it follows that $[P_1^\dagger P_1, U] = 0$. This assures that $\hat{U} := P_1 U P_1^\dagger$ is unitary. It commutes with \hat{R}_0 and hence also with $\sqrt{\hat{R}_0}$ and $\sqrt{\hat{R}_0^{-1}}$. From $[R_0, U] = 0$ and the previous facts, it follows that \hat{U} commutes with \hat{L}_0 . Using the same argument it follows

that $[P_2^\dagger P_2, \hat{U}] = 0$ showing that $U' = P_2 \hat{U} P_2^\dagger$ is unitary. Combining everything it follows that $U'V = VU$ and $U'W = WU$ showing that $[W^\dagger V, U] = 0$.

In order to show that Eq. (22) holds for any pair of fixed points R and L of \mathbb{T} we will first show that the support and range of any fixed point R of \mathbb{T} is contained in the support of R_0 . Let R be some Hermitian fixed point, and let $\epsilon > 0$ be sufficiently small such that $\mathbb{1} \pm \epsilon R$ is positive definite. The fixed point $\mathbb{T}^\infty(\mathbb{1} \pm \epsilon X) = R_0 \pm \epsilon R$ has to be positive by definition of CP, but the r.h.s. fails to be positive as soon as R has support outside R_0 . Since the fixed point space is closed under Hermitian conjugation (both $R + R^\dagger$ and $i(R - R^\dagger)$ are also fixed points for any non Hermitian R) the support and range of any fixed point R is contained in the support of R_0 .

From the restriction of the support and range of fixed points it follows that

$$\begin{aligned}
\text{Tr}(L^\dagger R) &= \text{Tr}(L^\dagger P_1^\dagger P_1 R P_1^\dagger P_1) \\
&= \text{Tr}(\sqrt{\hat{R}_0} P_1 L^\dagger P_1^\dagger \sqrt{\hat{R}_0} \sqrt{\hat{R}_0^{-1}} P_1 R P_1^\dagger \sqrt{\hat{R}_0^{-1}}) \\
&= \text{Tr}(P_2^\dagger P_2 \sqrt{\hat{R}_0} P_1 L^\dagger P_1^\dagger \sqrt{\hat{R}_0} P_2^\dagger P_2 \cdot \\
&\quad \sqrt{\hat{R}_0^{-1}} P_1 R P_1^\dagger \sqrt{\hat{R}_0^{-1}}) \\
&= \text{Tr}(W L^\dagger W^\dagger V R V^\dagger) .
\end{aligned} \tag{A.3}$$

The third equality follows from the fact that the support and range of any fixed point L of \mathbb{T}^* is contained in the support of L_0 and hence that the support and range of $\sqrt{\hat{R}_0} P_1 L P_1^\dagger \sqrt{\hat{R}_0}$ is contained in the support of \hat{L}_0 . In more detail let $v \in \text{kern}(\hat{L}_0) \Rightarrow v \hat{L}_0 v = 0$ from which it follows (due to positivity of L_0) that $P_1^\dagger \sqrt{\hat{R}_0} v \in \text{kern}(L_0) \subset \text{kern}(L)$. Thus the support of $\sqrt{\hat{R}_0} P_1 L P_1^\dagger \sqrt{\hat{R}_0}$ is contained in the support of \hat{L}_0 . The restriction on its range follows from the invariance of the fixed point space under Hermitian conjugation.